Robert Corriu
Peter Jutzi
(Eds.)

Tailor-made Silicon-Oxygen Compounds

From Molecules to Materials

vieweg

Die Deutsche Bibliothek – CIP-Einheitsaufnahme

Tailor-made silicon oxygen compounds: from molecules to materials / Robert Corriu; Peter Jutzi (ed.). – Braunschweig; Wiesbaden: Vieweg, 1996
ISBN 3-528-06798-5

NE: Corriu, Robert [Hrsg.]

Produced by Lengericher Hubert & Co., Göttingen
Printed in the Federal Republic of Germany

ISBN 3-528-06798-5

12 Octasilasesquioxanes

Gion Calzaferri

Institute for Inorganic and Physical Chemistry
University of Berne, Freiestrasse 3
CH-3000 Bern 9, Switzerland

Abstract: Octasilasesquioxanes show a cube-shaped Si_8O_{12} unit. We distinguish between the spherosiloxane molecules, the ionic silicates $(X^+)_8(Si_8O_{20})^{8-}$, and the Si_8O_{12} cages present in polymeric materials. While a respectable number of $R_8Si_8O_{12}$ compounds are known, only a few $R'R_7Si_8O_{12}$ and even less $R'_2R_6Si_8O_{12}$ and $R'R''R_6Si_8O_{12}$ have been isolated so far. The crystal structures of n-hexyl-$H_7Si_8O_{12}$, phenyl-$H_7Si_8O_{12}$, and $Co(CO)_4$-$H_7Si_8O_{12}$ and the vibrational structure of them and also of styryl-$H_7Si_8O_{12}$ and phenyl-$H_7Si_8O_{12}$ were examined in detail. The best studied octasilasesquioxane molecule is $H_8Si_8O_{12}$. Its crystal-, vibrational-, and electronic structure were investigated in detail. $H_8Si_8O_{12}$ + Y-Z → $YH_7Si_8O_{12}$ + HZ etc. substitution reactions under retention of the cage are available and it seems that they are of radical type. O_h-$H_8Si_8O_{12}$ is an excellent molecule for introducing the notion of ring opening vibrations. They open a gate for studying the pore opening vibrations which are believed to play an important role in the dynamics and the transport properties of zeolites. It is amazing that among the many orbitals of O_h-$H_8Si_8O_{12}$ there is exactly one of A_{2g} symmetry. This pure oxygen-lone pair, which cannot interact with AOs from other centres than oxygen, is the highest occupied orbital (HOMO), followed by a number of oxygen lone pairs between -10.75 and -11.7 eV which interact only slightly with the Si atoms. $H_8Si_8O_{12}$ was shown to be useful to improve our understanding of the electronic nature of extended structures by comparing its properties with those of α-quartz and with the results of band structure and density of states calculations of the silicon dioxide analogue of zeolite A. $R'R''R_6Si_8O_{12}$ molecules are very attractive for building structurally well defined donor/acceptor systems D/A in which the distance between D and A is varied by the number of intervening groups in a molecular bridge. It would be very interesting to have such molecules at hand. The Si-O-Si bridge is not well understood but quantumchemical calculations indicate that through bond interactions over short bridges range from isolating behaviour to significant coupling, depending on the nature of the substituents and on the conformation.

12.1 Introduction

Octasilasesquioxanes with the general formula $R_8Si_8O_{12}$, $R_7R'Si_8O_{12}$ etc. show a cube-shaped Si_8O_{12} unit as illustrated in Figure 1. They are probably the best studied members of the large class of silasesquioxanes $(RSiO_{3/2})_{2n}$, n=1,2,3 etc., which has attained much interest in the last few years. We distinguish between the spherosilioxanes, the ionic silicates $(X^+)_8(Si_8O_{20})^{8-}$ and the Si_8O_{12} cages present in polymeric materials. All or some of

the Si can be replaced by other tetrahedrally co-ordinated atoms such as Al, P, Ga or Ge to obtain the T_8O_{12} cages occurring in several zeolites as "double-4-ring" D4R secondary building units [1]. The silicate [2,3] $[Si_8O_{20}]^{8-}$ and the aluminosilicate anions [4,5] $[(Al_4Si_4O_{12})(OH)_8]^{4-}$ have been well characterized. They play a role as intermediates in the synthesis of some zeolites [2-6]. A T_8O_{12} cage of $[(RSi)_4(R'Ti)_4O_{12}]$ composition was reported recently [7].

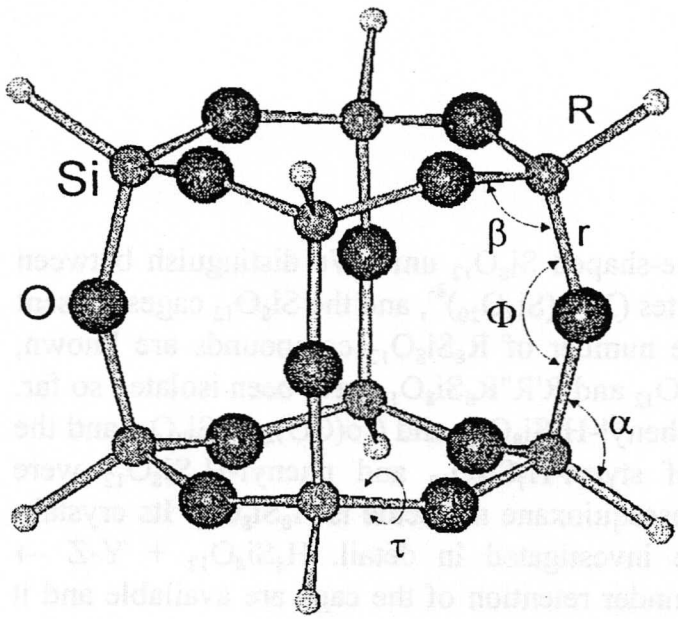

Figure 1: Structure of the (-Si)$_8O_{12}$ cage. R, r, α, β, ϕ, and τ are the internal coordinates.

The first octaspherosiloxane molecule, $(CH_3)_8Si_8O_{12}$, can be traced back to Scott who reported in 1946 the synthesis of $(CH_3SiO_{3/2})_{2n}$ compounds which he was, however, not able to further identify because of solubility problems [8]. Müller et al. described the preparation of $H_8Si_8O_{12}$ crystals in 1959 and made the right guess of its structure [9]. Larsson published an X-ray analysis of $R_8Si_8O_{12}$ (R = CH_3, n-C_3H_7, i-C_3H_7, Phenyl, and H) in three papers in 1960 [10]. Additional $R_8Si_8O_{12}$ were prepared and studied during the following years [11], but larger interest in spherosiloxanes and especially octaspherosiloxanes started after 1985. Since then an increasing number of $R_8Si_8O_{12}$, some $R'R_7Si_8O_{12}$, and a few $R'_2R_6Si_8O_{12}$ and $R'R''R_6Si_8O_{12}$ compounds have been synthesized. An overview is given in Table 1. Some of these compounds have been discussed as building blocks for the preparation of highly silicic materials or as starting molecules for new organosiliceous polymers. Recently, stable encapsulation of atomic hydrogen upon γ-irradiation of $[(CH_3)_3SiO]_8Si_8O_{12}$ was reported [12]. Among the $R_8Si_8O_{12}$ molecules, $H_8Si_8O_{12}$ has especially attracted our interest [13]. It is a stable molecule which can be prepared easily in good yield by acidic hydrolysis of $SiHCl_3$ in a biphasic solution in presence of $FeCl_3$ [14]. We have shown that it is an ideal model for obtaining information on the electronic [15], the vibrational [16,17], and the crystal structure of more extended siliceous materials [1]. It turned out to be a suitable starting molecule for synthesizing mono and higher substituted octanuclear silasesquioxanes [18-27]. $H_8Si_8O_{12}$ and also other hydrospherosiloxanes were recently discussed as precursors for atomic scale control of the Si/SiO_2 interface [28].

Table 1: Octasilasesquioxanes reported in the literature, an overview.

$R_8Si_8O_{12}$	R=	References
	H	[11]
	CH_3, C_2H_5, C_3H_7, $CHMe_2$, C_4H_9, C_5H_{11}, C_6H_{13}, i-C_9H_{19}, C_6H_{11}, $CH{=}CH_2$, $CH_2CH{=}CH_2$	
	C_6H_5, 4-Tolyl, X-$NO_2C_6H_4$, 1-Naphtyl	
	2-C_4H_3S, 2-C_4Br_3S	
	$OSiMe_3$, $ONMe_4$ (= $[NMe_4^+]_8[Si_8O_{20}]^{8-}$)	
	Cl, OMe	[18]
	$OSiMe_2CH{=}CH_2$, $OSiMe_2CH_2CH{=}CH_2$,	[29]
	$OSiMe_2H$	[30]
	p-$C_6H_4CH_2X$, X=I, OH,ONO_2, OAc, p-Nitrobenzoyl, Methylterephthaloyl, $OPPh_2$, $P(O)Ph_2$, PPh_2	[31]
	$OSiMe_2CH_2Cl$	[32,33]
	D	[19]
	$OSnMe_3$, $OSbMe_4$	[34]
	$CH_2C_6H_{11}$	[20]
	2-$C_6H_4NMe_2$	[35]
	(η-C_5H_5)Fe(η-$C_5H_4CH_2CH_2$-)$SiMe_2O$–	[36]
	$C_{10}H_{21}$, $C_{14}H_{29}$, $C_{18}H_{36}$, $C_4H_9[SiMe_2O]_3SiMe_2CH_2CH_2$-, $C_4H_9[SiMe_2O]_3SiMe_2CH_2CH_2CH_2$-,	[37]
	$CH_2CH_2CH_2X$, X=Cl, I, SH, SMe, -CN, -SCN, $SiMe_3$, C_6H_5, -OC_4H_9, -$SO_2C_6H_4$, -OC_6H_5, $P(C_5H_5)_2$	[27]
	(-O-$SiMe_2(CH_2CH_2X)$, X = $CH_2(C_2Me)B_{10}H_{10}$, $C_5H_3MeMn(CO)_3$, $SiMeC_5H_4FeC_5H_5$, $SiMeCl_2$, $Si(OEt)_3$	[38]
$R'R_7Si_8O_{12}$	R =...; R'	
	H; $CH_3(CH_2)_4CH_2$-, $C_6H_5CH_2CH_2$-	[21]
	H; [η-C_5H_5)Fe(η-$C_5H_4CH_2CH_2$)]-	[22]
	H; $Co(CO)_4$	[23]
	H; $C_6H_5CH{=}CH$-	[24]
	H; $C_{10}H_7CH_2CH_2$-, $C_{14}H_9CH_2CH_2$-, -O-(HSi_8O_{12})	[39]
	H; C_6H_5	[40]
	$HSiMe_2O$;[η-C_5H_5)Fe(η-$C_5H_4CH_2CH_2$-)$SiMe_2O$-	[36]
	CH_3CH_2; [$Cr(CO)_3$]$C_6H_5CH_2CH_2$-	[39]
	C_3H_7; 3-ClC_3H_6, 3-IC_3H_6, 3-HSC_3H_6, C_3H_5	[26]
	CH_3CH_2; C_2H_3	
	c-C_7H_{13}, c-C_6H_{11}, and c-C_5H_9; methylacrylate	[41]
	c-C_6H_{11}; [...-O-($AlSi_7O_{12}$)$R'_7]^-[Me_4Sb]^+$	[42]
	c-C_6H_{11}; H, Cl, -$CHPMe_3$, -$CHPPh_3$	[43]

$R'R''R_6Si_8O_{12}$ R=...; (R', R'')		
	CH_3CH_2; (ϕ -CH=CH-)$_2$, ((ϕ-CH=CH-, ϕ-(C-...)=CH_2), different isomers	[25,44]
	C_3H_7; (3-ClC_3H_6)$_2$, (3-IC_3H_6)$_2$, (3-HSC_3H_6)$_2$, (C_3H_5)$_2$	[26]
	CH_3CH_2; (C_2H_3)$_2$	
Some others		
	($OSnMe_3$)$_{8-n}$($OPCl_2$)$_p$(O_2PCl_q), n=2q+p	[45]
	($Me_nSi_8O_{20-n}$)$^{(8-n)-}$, n=1,2,3	[46]
	Polymers containing (Si_8O_{20}) units	[47]

12.2 Synthesis of octaspherosiloxane molecules

A general procedure to prepare spherosiloxanes is polycondensation of trifunctional $RSiX_3$ monomers, X = Cl or OR. Synthesis of an aminoorganyl substituted ocatasilasequioxane starting from a zwitterionic λ^5.spirosilicate was recently reported [35]. It is remarkable that the first Si-X substitution reaction $X_8Si_8O_{12}$ + Y-Z → $Y_8Si_8O_{12}$ + 8XZ (X = H or Cl, Y = Cl, $OSiMe_3$ or OCH_3) was reported by Klemperer and co-workers as late as 1985 [18]. Reactions of the silicates $(X^+)_8[Si_8O_{20}]^{8-}$ which are eg. used to prepare $[(CH_3)_3SiO]_8Si_8O_{12}$ have been known much longer [29]. We deuterated $H_8Si_8O_{12}$ completely [19] and we found that hydrosilation of methylenecyclohexane and of hex-1-ene by $H_8Si_8O_{12}$ catalysed by hexachloroplatinitic acid leads quantitatively to the corresponding $R_8Si_8O_{12}$ product [20]. Hydrosilation was successfully applied for the preparation of a number of mono- and disubstituted $R'R_7Si_8O_{12}$ and $R'R''R_6Si_8O_{12}$ molecules [21,22,24-27,39,40]. The first octasilasesquioxane with a Si-metal bond, $[Co(CO)_4]H_7Si_7O_{12}$, was obtained by reacting $[Co_2(CO)_8]$ with $H_8Si_8O_{12}$ according to [23].

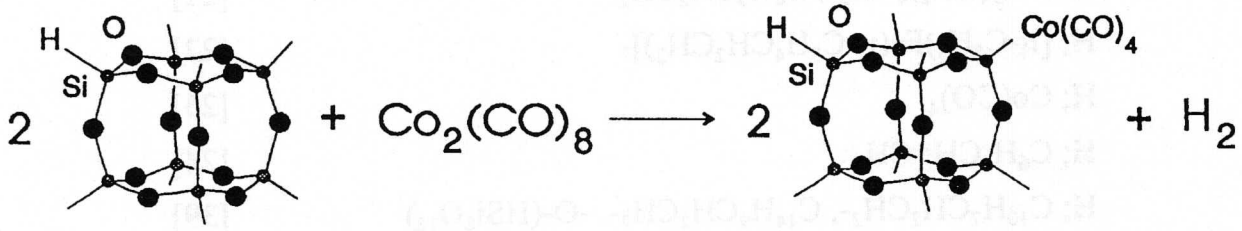

Scheme I

This means that substitution reactions under retention of the cage structure are available and this might be used for stereoselective reactions. It seems that the mechanism of the so far

known $X_8Si_8O_{12} + Y\text{-}Z \rightarrow YH_7Si_8O_{12} + XZ$ etc. reactions is of radical type and that it can be described by Scheme II.
This is based on a theoretical study of the deuteration $H_8Si_8O_{12} + D_2 \rightarrow D_8Si_8O_{12}$ and on the observation that all attempts to apply nucleophilic substitution results in destruction of the cage [15].

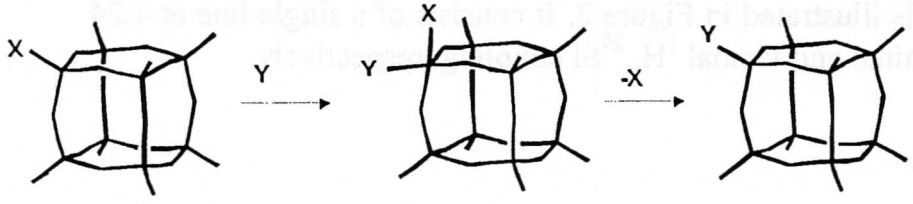

Scheme II

Three general ways for synthesizing monosubstituted $R'R_7Si_8O_{12}$ molecules have been used so far. They are summarized in Scheme III.

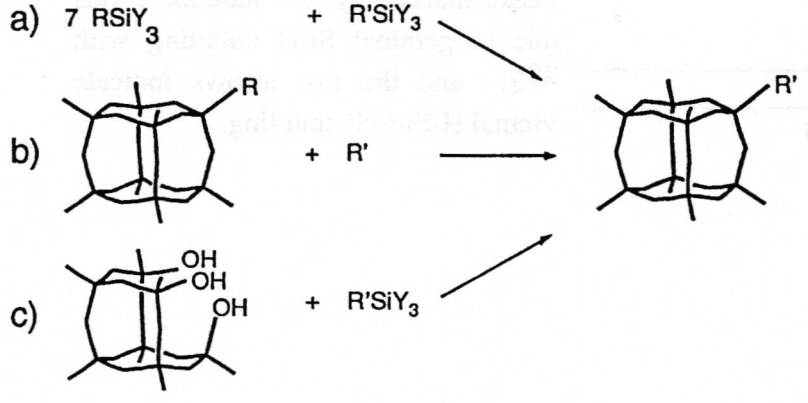

Scheme III

a) The classical route to spherosiloxanes is polycondensation of trifunctional $RSiY_3$ monomers. We have applied it for the synthesis of the monophenylsilasesquioxanes C_6H_5-$(H_{n-1}Si_nO_{1.5n})$ n=8 and 10 which cannot be prepared by hydrosilation [40]. b) is probably the most generally applicable principle because of the easy availability of $H_8Si_8O_{12}$ and most of the known mono and disubstituted $R'R_7Si_8O_{12}$ and $R'R''R_6Si_8O_{12}$ have been prepared in this way. It can also be applied to other hydrosilasesqioxanes such as $H_{10}Si_{10}O_{15}$. a) and b) lead to mixtures which can be separated by HPLC. c) was developed by Feher. It has the advantage of leading to one product only [43].

12.3 $H_8Si_8O_{12}$ - an ideal model compound

$H_8Si_8O_{12}$ is a stable molecule. It crystallizes in n- or c-hexane to give colourless needles which sublime at ambient pressure with a sublimation enthalpy and temperature of ΔH_{subl} = 98.5 kJ/mol and T_{subl} = 206 °C, respectively. Its crystal structure was studied in much detail with special emphasis on the flexibility of the Si-O-Si bridge. T_h symmetry for the Si_8O_{12} framework and S_6 symmetry for the eight H atoms were found in the crystalline state [48,49]. A systematic investigation of structural distortion in Si_8O_{12} fragments and D4R units lead to the result, that most of the deformations observed in T_8O_{12} correspond to those

expected from a model of rigid tetrahedra joined flexibly across corner-sharing oxygen atoms [1]. The symmetry deformation coordinates found to be important in the analysis of static distortions are the same as the coordinates associated with the six lowest vibrational frequencies of $H_8Si_8O_{12}$, namely the δ(Si-O-Si) E_g at 83 cm^{-1}, the δ(Si-O-Si) T_{2u} at 68 cm^{-1} and the τ_{as}(Si-O-Si) A_{2g} at 53 cm^{-1} reported in Table 2. Raman [16] and INS (inelastic neutron scattering) [50] spectra of crystalline samples are fully compatible with the solid state structure while the IR as well as the ^1H and ^{29}Si NMR spectra indicate O_h symmetry in solution. The ^1H NMR spectrum is illustrated in Figure 2. It consists of a single line at 4.24 ppm. The satellites are due to geminal and vicinal ^1H, ^{29}Si coupling, respectively.

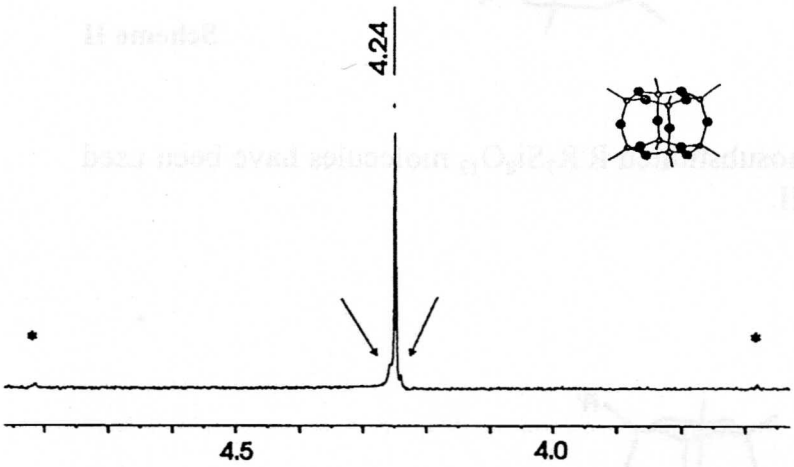

Figure 2: ^1H-NMR spectrum of $H_8Si_8O_{12}$ (300 MHz, $CDCl_3$, ppm). Peaks marked by a * indicate bands due to geminal Si-H coupling with ^{29}Si and the two arrows indicate vicinal H-Si-OSi coupling.

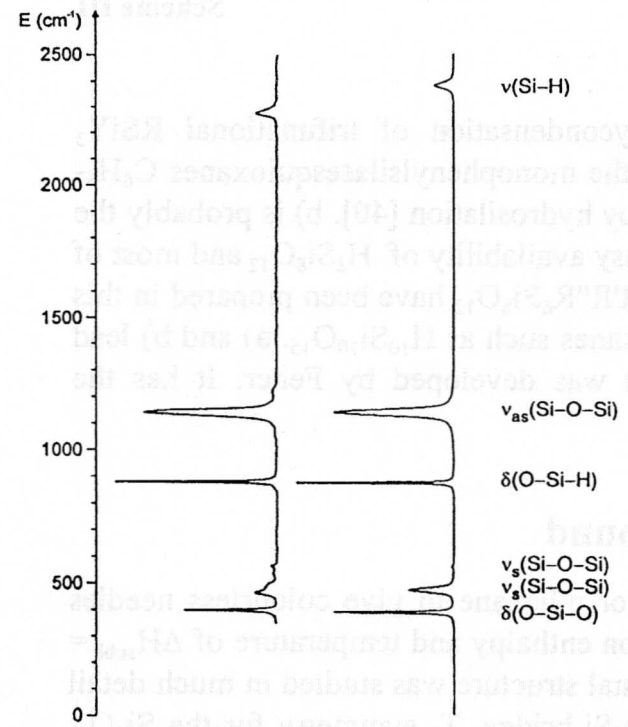

Figure 3: IR Transmission spectrum of $H_8Si_8O_{12}$. Left: Experimental spectrum measured in CCl_4 with a resolution of 0.5 cm^{-1}. Right: Calculated spectrum. It consists only of fundamentals while oveertone and combination bands are present in the experimental spectrum.

O_h-$H_8Si_8O_{12}$ possesses 78 vibrational degrees of freedom. From its symmetry follows that the IR spectrum consists of 6 fundamental IR active modes, all of T_{1u} type. The resulting bands are shown in Figure 3 and compared with a calculated spectrum based on an experimental force field determined by us [16]. The calculated bands of the fundamentals are in close agreement with the observed frequencies and relative intensities. Harmonic correction of the experimental Si-H stretching frequencies shifts them close to the calculated values. This means that the force field is good, a conclusion which is supported by the data given in Table 2 were the experimental IR, Raman and INS fundamentals are compared with the calculated frequencies [50,51].

We have already stated that the IR spectrum as well as the ^1H and ^{29}Si NMR measurements indicate for $H_8Si_8O_{12}$ in solution O_h symmetry while X-ray and neutron diffraction of crystals show T_h for the Si_8O_{12} framework and S_6 for the H atoms. Column I of Table 2 shows the results of the calculation in O_h symmetry. Column II is based on S_6 symmetry which splits the O_h-T_{1g} band at 865 cm^{-1} in an A_{1g} and an E_g vibration at 865 and 815 cm^{-1}, respectively, and the E_u vibration at 862 cm^{-1} shifts to 815 cm^{-1}, in full agreement with the experiment, for details see refs. [16,17,51]. It was also shown that the force field determined for $H_8Si_8O_{12}$ is appropriate to describe the fundamentals of $H_{10}Si_{10}O_{15}$ [17,52].

We observed that $H_8Si_8O_{12}$ is an excellent starting point for studying the pore opening vibrations which are believed to play an important role in the dynamics and the transport properties of zeolites. A relation between $H_8Si_8O_{12}$ and $H_{24}Si_{24}O_{36}$ and the structure of Zeolite A is shown in Figure 4. Since $H_{24}Si_{24}O_{36}$ bears the structure of the sodalite cage, it may be used as a link to the many zeolites in which this structure is present. Several attempts were made to assign the observed vibrational modes to specific local structural features of zeolites and especially to pore opening vibrations. We have introduced the notion of ring opening vibrations (ROVI) of hydrosilasesquioxanes. Based on this we suggested a new way to study the pore opening vibrations of zeolites which simplifies the problem remarkably and thus leads to a better understanding of the more complex extended structures [17].

Table 2: Normal mode frequencies / cm^{-1} of $H_8Si_8O_{12}$ [50,51].

	experimental			calculated	
Symmetry	IR	Raman	INS	I	II
A_{1g}		2302	2301	2381	2381
T_{2g}		2286/2296	2301	2381	2381
T_{1u}	2277		2301	2381	2381
A_{2u}			2301	2381	2381
T_{1g}				1161	1161
E_u				1158	1158
T_{1u}	1141			1143	1143
T_{2g}		1117		1116	1115/1116
A_{2u}				1082	1081
E_g		932	916	922	916

	experimental			calculated	
Symmetry	IR	Raman	INS	I	II
T_{2u}			916	918	908/918
T_{2g}		883/897	879/890	890	882/894
T_{1u}	881		870/879	881	871/881
T_{1g}		811.	817/870	865	815/865
E_u			817	862	815.
E_g		697.	688	691	686.
T_{2u}			675	682	676/682
T_{2g}		610.	608	613	611/613
A_{1g}		580.	563	576	573.
T_{1u}	566		563	569	566/569
T_{1u}	465		458	481	477/481
A_{1g}		456.	458.	446	446.
E_g		423.	415.	423	423.
T_{2g}		414.	400/405	418	413/418
T_{1u}	399		389.	397	397.
T_{1g}		352.	330.	356	355/356
A_{2u}			314.	304	303.
T_{2u}			286.	303	302.
T_{2g}		171.	175/178	168	167.
E_u			172.	166	166.
E_g		84.	88.	83	83.
T_{2u}			65.	68	68.
liberation			49/54		53.
A_{2g}			40.		
translation			20.		

The ROVI are normal modes in which all Si-O stretching and/or O-Si-O angle bending displacements of the considered ring are in phase. The symmetry species of these modes are determined by the new sets of coordinates illustrated in Figure 5 for the hexaeder which represents the Si_8 cage of $H_8Si_8O_{12}$. Each arrow is a representation of the corresponding 4-ring opening perpendicular to it. The displacements of these coordinates are breathing motions of the ring. This leads to the representations (1) for O_h-$H_8Si_8O_{12}$ and (2) for O_h-$H_{24}Si_{24}O_{36}$ in which RO stands for ring opening. 4R and 6R symbolize the Si_4O_4 and the Si_6O_6 rings, which are in fact 8- and 12-rings, respectively.

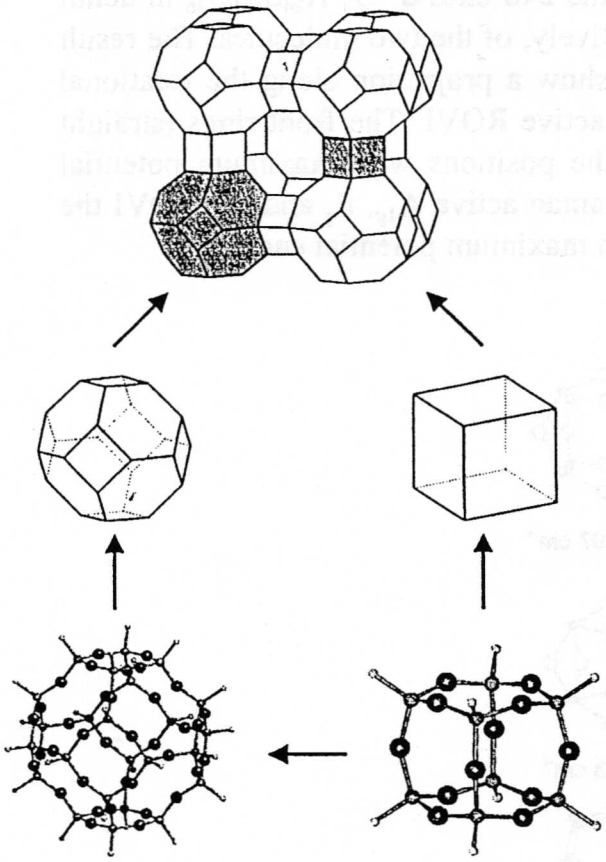

Figure 4: Relation between $H_8Si_8O_{12}$ and $H_{24}Si_{24}O_{36}$, between $H_8Si_8O_{12}$ and the 4DR of Zeolite A, and between $H_{24}Si_{24}O_{36}$ and the β-cage.

$H_8Si_8O_{12}$:

$$\Gamma_{RO}^{4R} = A_{1g} + E_g + 2T_{1u} \tag{1}$$

$H_{24}Si_{24}O_{36}$:

$$\Gamma_{RO}^{4R} = A_{1g} + E_g + 2T_{1u} \tag{2}$$

$$\Gamma_{RO}^{6R} = A_{1g} + 2T_{2g} + A_{2u} + 2T_{1u}$$

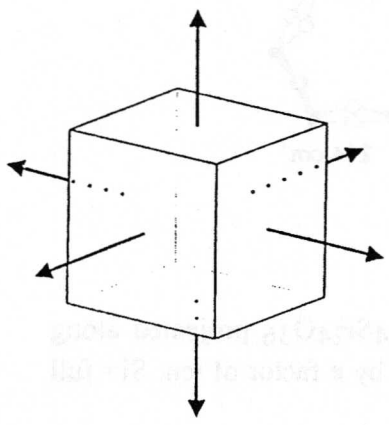

Figure 5: Set of equivalente coordinates defining the ring opening vibrations (ROVI) of a cube, especially O_h-(-Si_8O_{12}).

Analysing the 78 normal modes of O_h-$H_8Si_8O_{12}$ and the 246 ones of O_h-$H_{24}Si_{24}O_{36}$ in detail allowed us to identify the 9 and the 19 ROVI, respectively, of the two molecules. The result of this analysis is illustrated in Figure 6 where we show a projection along the rotational axis perpendicular to the ring of the IR and Raman active ROVI. The front rings (straight lines) and the back rings (dashed lines) represent the positions with maximum potential energy in case of the IR active T_{1u} modes. For the Raman active A_{1g}, E_g and T_{2g} ROVI the two rings represent the positions of the front ring with maximum potential energy.

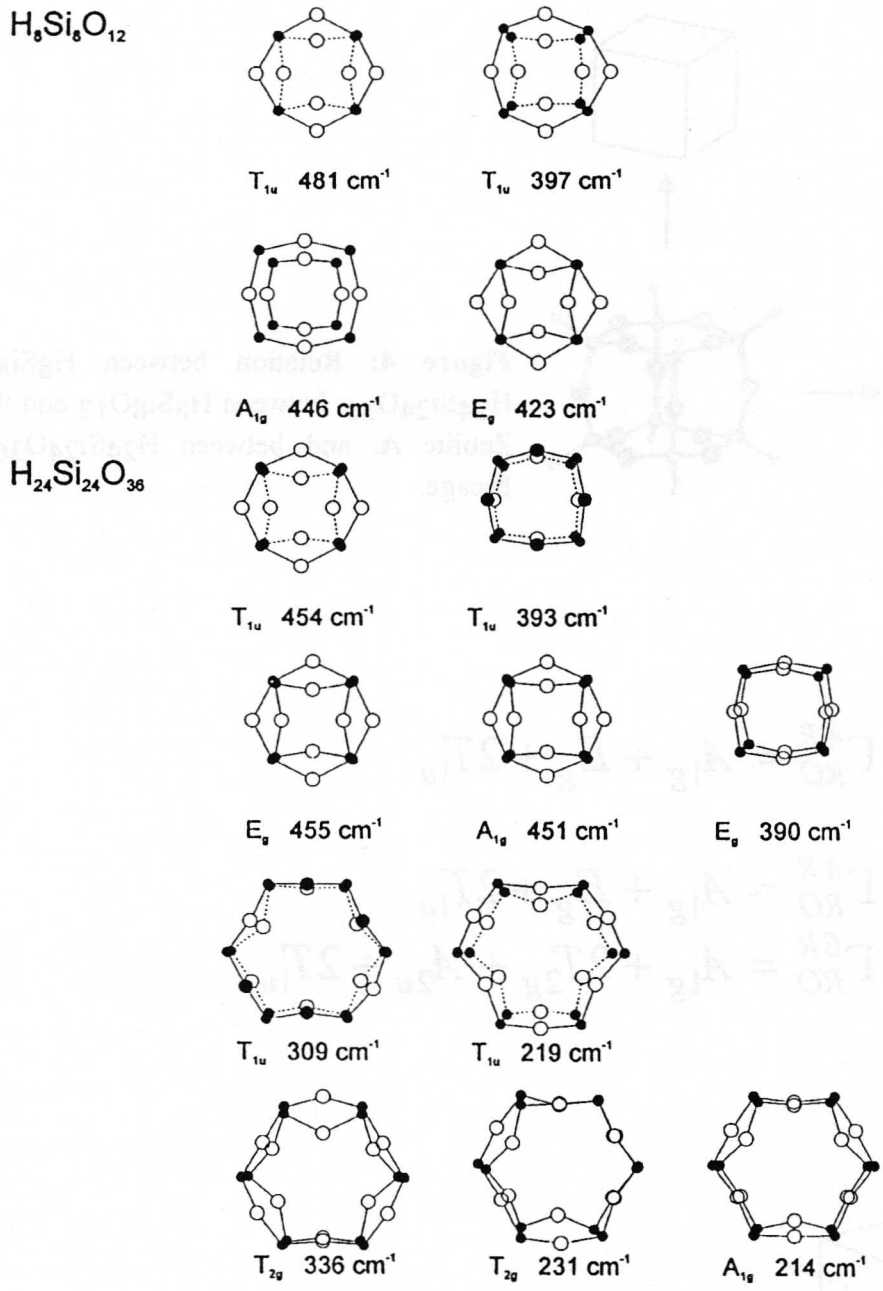

Figure 6: Ring opening vibrations (ROVI) of O_h-$H_8Si_8O_{12}$ and O_h-$H_{24}Si_{24}O_{36}$ projected along the rotational axis perpendicular to the ring. The amplitudes are magnified by a factor of ten. Si= full circles, O=open circles.

The energy of the 4- and of the 6-ring ROVI are within a range of 90 cm^{-1} (481-390 cm^{-1}) and (309-214 cm^{-1}) respectively, and the 6-rings vibrate at lower energy than the 4-rings. This result improves our understanding of the 4- and of the 6-ring pore opening vibrations of zeolites [16,17]. It is amazing that among the many orbitals of O_h-$H_8Si_8O_{12}$ there is exactly one of A_{2g} symmetry [15]. This pure oxygen-lone pair, which cannot interact with AOs from other centres than oxygen, is the highest occupied orbital (HOMO), followed by a number of oxygen lone pairs between -10.75 and -11.7 eV which interact only slightly with the Si atoms. The HOMO-LUMO (lowest unoccupied molecular orbital) energy gap is in the order of 12 eV. A comparison of the calculated one-electron energy levels in the HOMO region and the measured photoelectron spectrum is illustrated in Figure 7. The calculated first ionization potential of 10.7 eV is low but in good agreement with the experimental observation. To get a feeling for the consequences of this relatively high lying HOMO, we compare it with the first ionization energy of water, observed at 12.6 eV and attributed to the energy of the p-type oxygen lone pair of the water molecule [53].

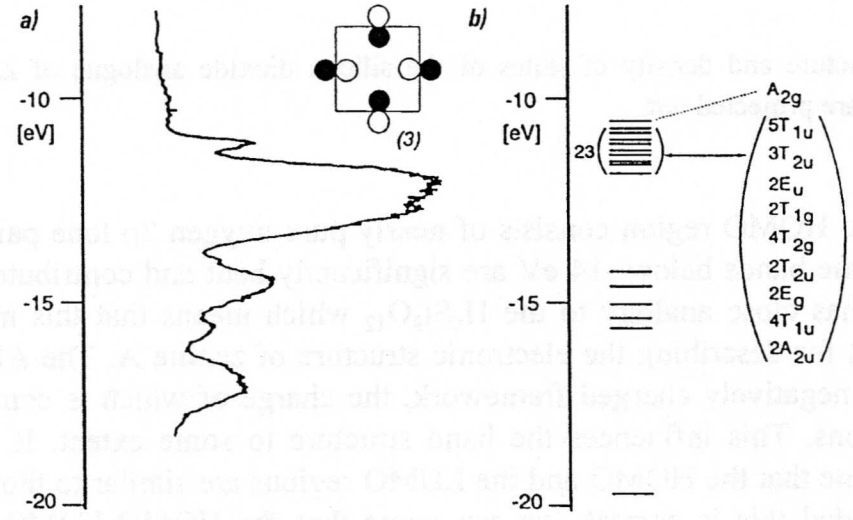

Figure 7: Photoelectron spectrum of $H_8Si_8O_{12}$ (a) and calculated one-electron levels (b). The A_{2g} symmetry of the HOMO localized at the O atoms is indicated.

We note that the first ionization potential of α-quartz is 10.4 eV, as determined by valence-band spectroscopy [54]. We have discussed the link of $H_8Si_8O_{12}$ to zeolites from point of view of vibrations. A similar link is useful for improving our understanding of the electronic properties of extended structures [55]. In Figure 8 we illustrate the band structure and density of states of the silicon dioxide analogue of Zeolite A. We observe that the bands in the HOMO region are flat which indicates the presence of non bonding states. Further insight is gained from the density of states DOS(E), defined such that DOS(E)dE is the number of states in the interval E to E+dE. Since we are expressing the crystal orbitals as linear combination of atomic orbitals (LCAO) we can project out specific atomic orbitals or linear combinations of them. In Figure 8 this was done by shading the oxygen 2p contributions and leaving the 2s oxygen and the silicon contributions blank.

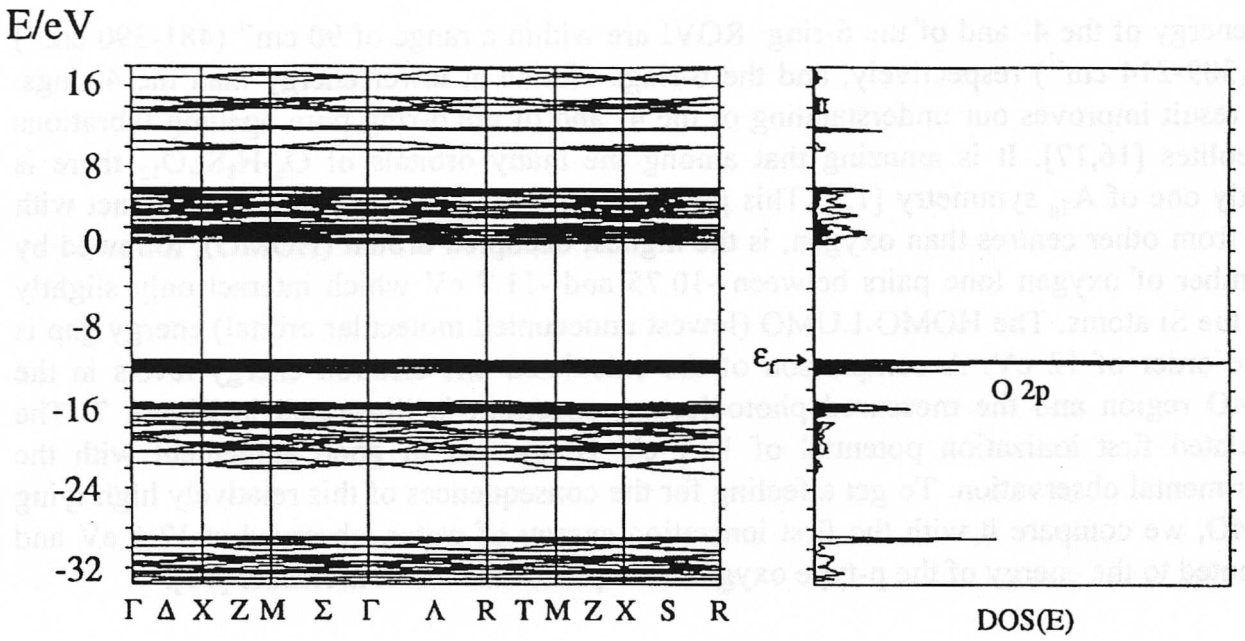

Figure 8: Band structure and density of states of the silicon dioxide analogue of Zeolite A. The oxygen 2p densities are projected out.

This shows that the HOMO region consists of nearly pure oxygen 2p lone pairs which we denote as $|O<$. Some bands below -14 eV are significantly bent and contribute to the Si-O bonding. All this has close analogy to the $H_8Si_8O_{12}$ which means that this molecule is a good starting point for describing the electronic structure of zeolite A. The Al^{3+} centres in Zeolite A cause a negatively charged framework, the charge of which is compensated by exchangeable cations. This influences the band structure to some extent. It is, however, reasonable to assume that the HOMO and the LUMO regions are similar to those illustrated in Figure 8. Provided this is correct, we can guess that the HOMO-LUMO region of a Zeolite A containing monovalent cations of the type Li^+,...,Cs^+, Cu^+, Ag^+, Au^+ can be drawn as illustrated on the left side of Figure 9. It consists of the oxygen lone pair region denoted as $|O<$, the empty ns' level of the metal cations M^+ and of the LUMO region of the zeolite which may be modified by np' contributions of M^+. The ns' and np' levels are modified to some extent with respect to the ns and np levels of the free cations by their interaction with the surrounding [56,57]. This scheme suggests the occurrence of ligand to metal charge transfer (LMCT) transitions of the ns'$\leftarrow|O<$ type, exciting an oxygen lone pair electron to the metal cation coordinated to the zeolite oxygen. The energy ΔE_{CT} needed for this transition is equal to the difference of the ionization potential $Ip_{|O<}$ of the oxygen lone pair and the first ionization potential Ip_M of the metal plus a correction Δ which stands for the antibonding interaction of the empty ns' level of the metal ion M^+ with the environment [13].

$$\Delta E_{CT}\,(ns' \leftarrow |O<) = I_{p|O<} - Ip_M + \Delta \qquad (3)$$

This simple relation allows us to compare the energy of the charge transfer band for different situations. We do this in Table 3 for cations in water and in a silicate with oxygen lone pairs at about 10.7 eV. Such transitions were assumed to be important in the

photochemical oxidation of water with visible light observe in Ag^+-A zeolite containing systems. We recently found, however, that Cl^- present in these systems, which leads to the formation of silver chloride, is important in the water oxidation reaction [58,59].

Table 3: Estimation of the ns'←|O< LMCT charge transfer transition energy ΔE_{CT} for the cations M^+ in water and in a silicate with $Ip_{ns'\leftarrow|O<}$ = 12.6 eV and 10.7 eV, respectively. Cu^+ and Au^+ ions in water are not stable. Au^+ is expected to be stable in dry zeolites but it has not yet been reported.

M	Ip_M / eV	ΔE_{CT}(ns'←|O<) −Δ / cm^{-1}	
		$Ipns'_{\leftarrow|O<}$ =12.6 eV	$Ip_{ns'\leftarrow|O<}$ =10.7 eV
Li	5.36	56'216	43'067
Na	5.12	60'326	44'183
K	4.32	66'778	51'454
Rb	4.16	68'078	52'745
Cs	3.87	70'407	55'083
Cu	7.68	39'679	24'356
Ag	7.54	40'808	25'485
Au	9.18	27'582	12'258

ns'←|O< charge transfer transitions have been observed in Cu^+-A, Cu^+-X and Ag^+-A zeolites in the region of 28.000 cm^{-1} [57,59]. This means that Δ is in the order of 0.5 eV or 4.000 cm^{-1}. Ag^+ in water absorbs at about 225 nm, in agreement with (3), but at the moment there is no further evidence available to support this equation which nevertheless may be regarded as a useful zero order approximation. Luminescence of the Cu^+-A, Cu^+-X and Ag^+-A zeolites after ns'←|O< excitation occurs at 500-700 nm, depending on the samples and the conditions [57,59]. This means that the Stokes shift is in the order of 8.000 cm^{-1}. Excitation of an electron from the oxygen lone pair level |O< into the empty ns' orbital of the metal cation causes formal reduction of M^+ to M^0.

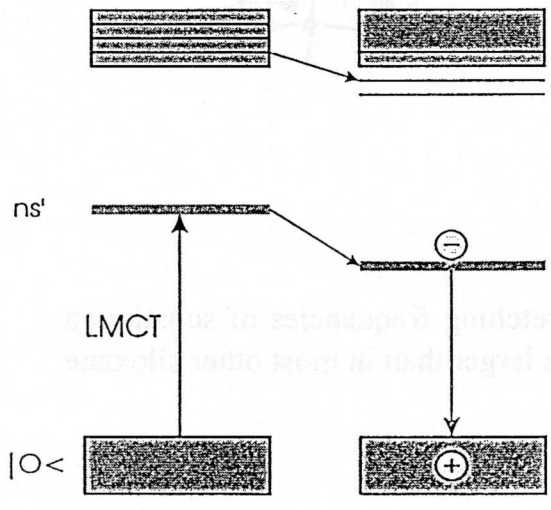

Figure 9: Development of the energy diagram of a metal cation in a silicate (zeolite) framework. The HOMO region consists of many closely spaced localized states strongly concentrated on the oxygen atoms. We call this region lone pair region of the silicate and abbreviate it as |O< . Some of the np' levels may reach into the LUMO region of the silicate. Three lines have been added to indicate this.

The radius r of M^+ is significantly smaller than that of M^0 ($r(Cu^+) = 0.96$ Å, $r(Cu^0) = 1.35$ Å, $r(Ag^+) = 1.26$ Å, $r(Ag^0) = 1.6$ Å).This means that the LMCT transition blows up the metal by $\Delta r \gg 0.3$-0.4 Å which has to change its position. As a consequence, the ns' level relaxes to a state of lower energy which we denote as $(|O<)^{\oplus}(ns')^1$ state [60]. It can relax to the ground state by emitting a photon with a large Stokes shift, as illustrated in Figure 9 on the right side.

12.4 $R'R_7Si_8O_{12}$ and $R'R''R_6Si_8O_{12}$ molecules

A few mono substituted $R'R_7Si_8O_{12}$ molecules have been synthesized within the last few years, see Table 1. The crystal and the vibrational structure of the three examples illustrated in Scheme IV has been investigated in detail [23,40,61]. It was found that the O-Si-O angles, α, are inversely proportional to the Si-O distances, d, and that the relationship conforms to the equation $d(Si\text{-}O)/Å = 1.59 + [1.6 \times 10^{-8}(180-\alpha)^4]$. The Si_8O_{12}-cage symmetry of $C_6H_{13}(H_7Si_8O_{12})$ lies closer to both C_{3v} and O_h than does $[Co(CO)_4(H_7Si_8O_{12})]$, and on average also closer to C_{3v} symmetry than $H_8Si_8O_{12}$ in crystals. The vibrational spectra of monosubstituted spherosiloxanes of the type $RH_7Si_8O_{12}$ can be understood as a superposition of the spectral features of $H_8Si_8O_{12}$ and of the substituent R. This was shown by phenomenological comparison of the IR and the FT-Raman spectra and by a detailed normal coordinate analysis [24,40,51,61]. It is illustrated in Figure 10 where we show the Raman spectrum of styryl-$H_7Si_8O_{12}$. The spectrum is divided into the lines assigned to the siloxane cage, the lines belonging to the substituent, and the vibrations involving the Si-C bond. This information may become useful, as the application rage of substituted spherosiloxanes increases.

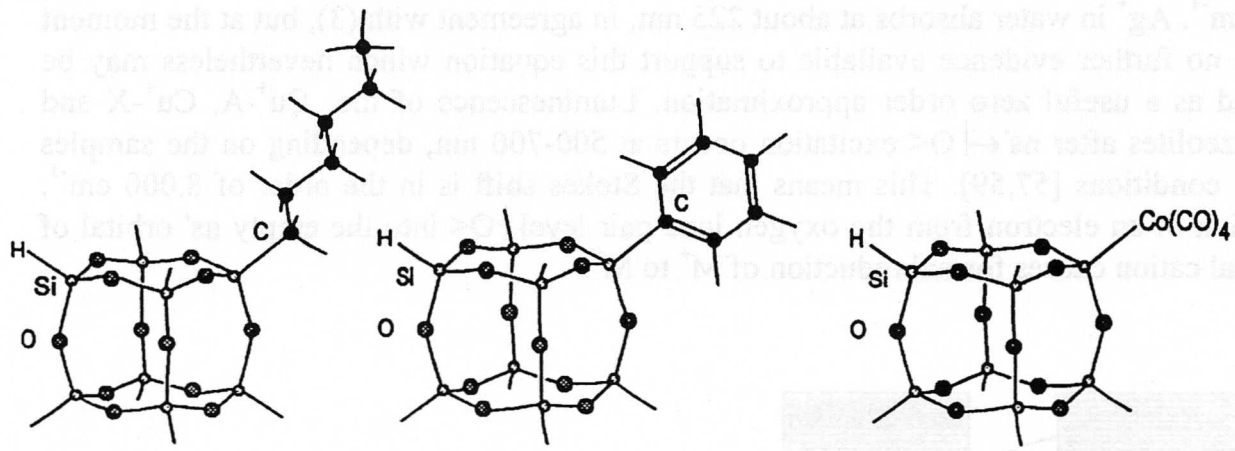

Scheme IV

In this context we note that the Si-H, Si-C and Si-Cl stretching frequencies of substituted and unsubstituted $R_8Si_8O_{12}$ molecules were observed to be larger than in most other siloxane compounds.

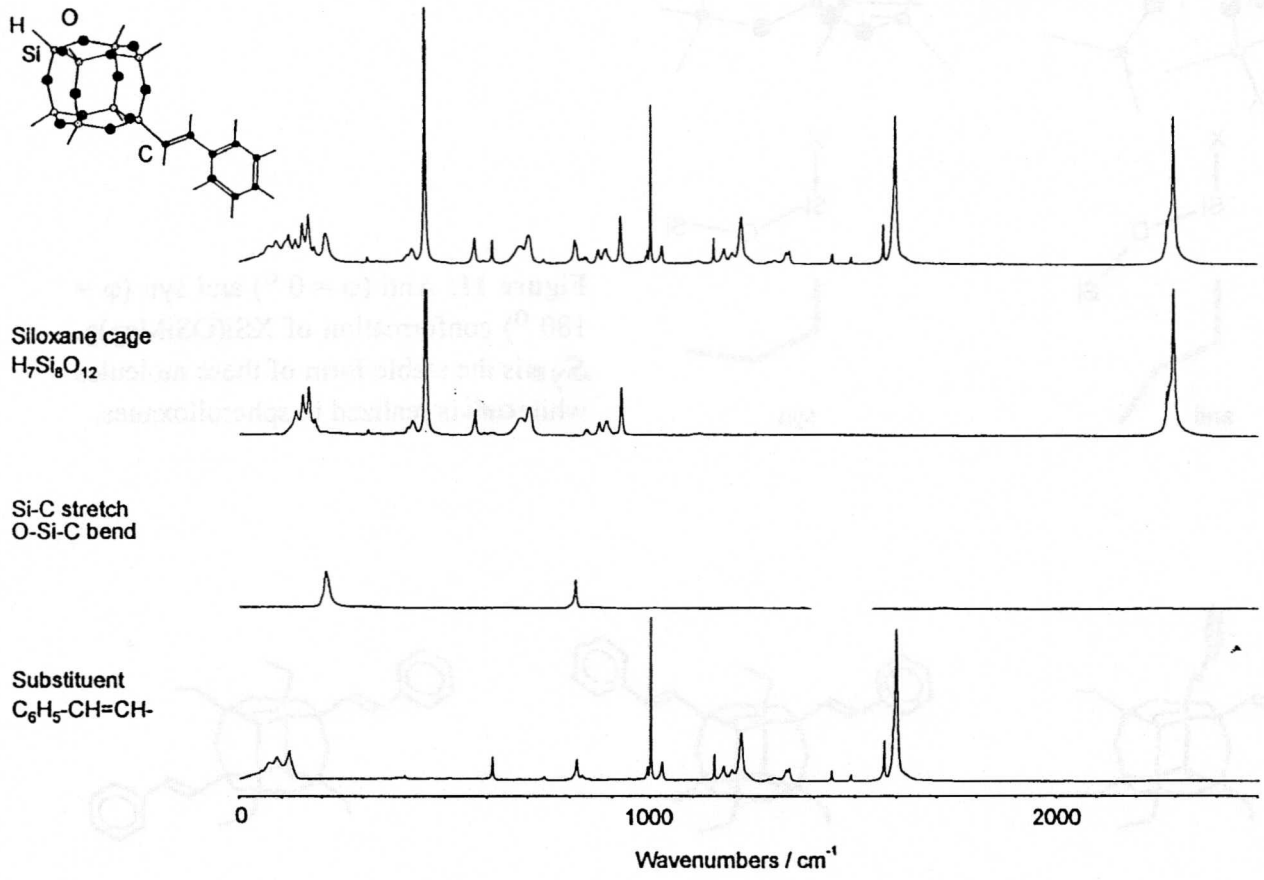

Figure 10: FT-Raman spectrum of styryl-$H_7Si_8O_{12}$, divided into the lines of the siloxane cage, of the substituent, and of the Si-C stretch and O-Si-C bend motion. The most intense peak in the spectrum of the $H_7Si_8O_{12}$ fragment is cut [24].

We found that this is due to the anti conformation present in the spherosiloxanes. An MO calculation on $XSi(OSiMe_3)_3$ (X=H, CH_3; Cl) in its syn and anti position illustrated in Figure 11 lead to the result that the Si-X bond order is significantly larger for anti than for syn [62].

Only a few $R'R''R_6Si_8O_{12}$ molecules have been synthesized in pure form, most of them by Marsmann et al. [26], see Table 1. Three $(F\text{-}CH{=}CH\text{-})_2(CH_3CH_2\text{-})_6Si_8O_{12}$ isomers which we characterized by NMR and MS are illustrated in Scheme V.

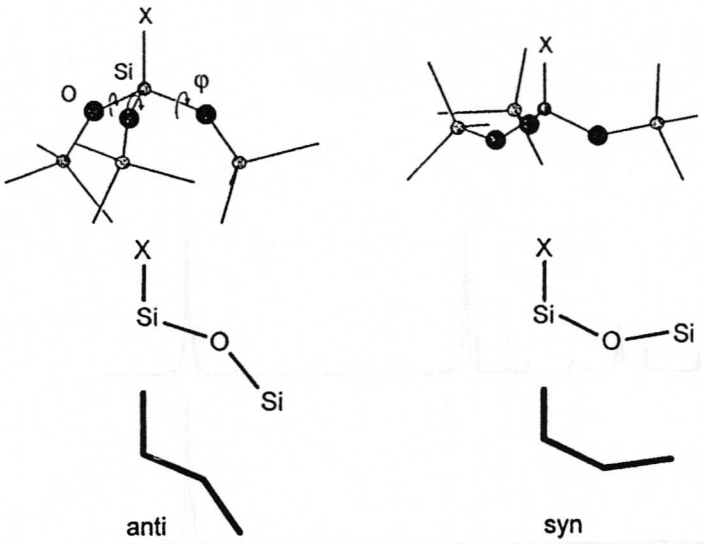

Figure 11: Anti ($\varphi = 0\ ^{o}$) and syn ($\varphi = 180\ ^{o}$) conformation of $XSi(OSiMe_3)_3$. Syn is the stable form of these moleules while anti is realized in spheroiloxanes.

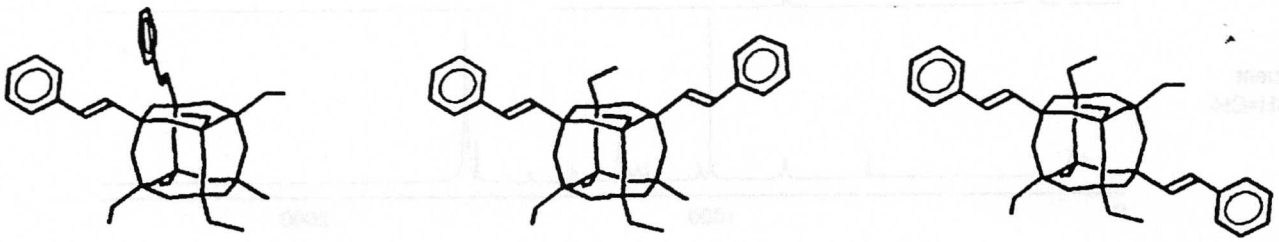

Scheme V

They were prepared by hydrosilation of phenylacetylene and separated by HPLC. The selectivity of the anti-Markovnikoff products was ~90% [25,44]. $R'R''R_6Si_8O_{12}$ molecules are very attractive for building structurally well defined donor/acceptor systems D/A of the type A-Si(OSi)$_n$OSi-D, n=0,1,2. In Scheme VI we illustrate the three octasilasesquioxane D/A isomers. It would be very interesting to have such molecules at hand. Since they have not yet been prepared we add a few theoretical considerations. Chemically linked D/A systems are used in studies of long-range trough-space and trough-bond interactions in the electronic ground and excited states [63,64].

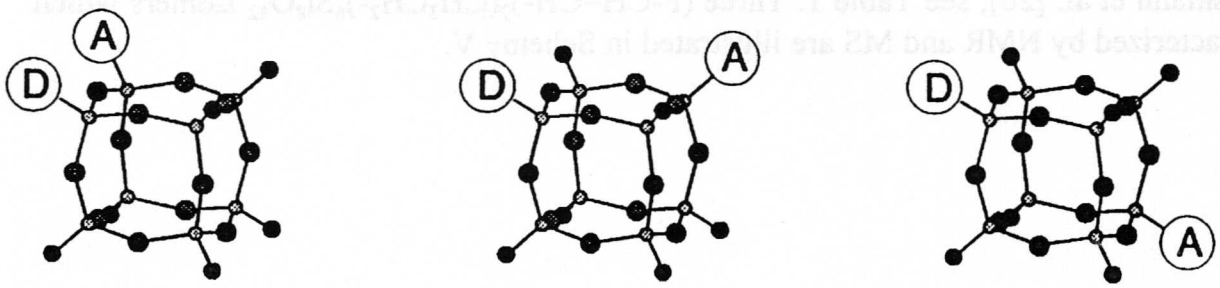

Scheme VI

The Si-O-Si bridge is not well understood so far but quantumchemical calculations indicate that through bond interactions over short bridges range from isolating behaviour to significant coupling, depending on the nature of the substituents and on the conformation. Such D/A systems can be compared with their purely organic analogues, based on eg. c-hexane bridges with naphthyl- and biphenyl- as donor and acceptor, respectively, which were studied in detail [65]. This comparison is illustrated in Scheme VII.

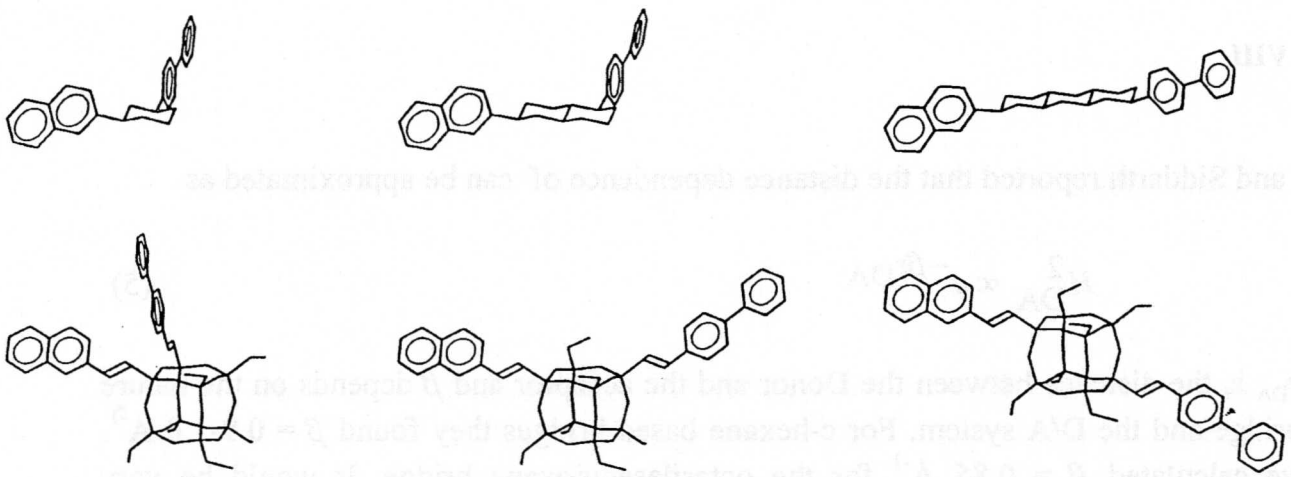

Scheme VII

According to our actual understanding the electron transfer rate constant k_{ET} from a donor D to an acceptor A can be described by

$$k_{ET} = H_{DA}^2 \times \text{Funktion of several parameters} \qquad (4)$$

H_{DA} describes the electronic coupling between the donor and the acceptor via the bridge. It can be calculated and the EHMO method has been found to be useful for this purpose [66]. Calculations on different D/A systems with an octasilasesquioxane bridge indicate that $|H_{DA}|$ ranges from zero to significant values, thus indicating that the properties of siloxane bridges ranges from insulating to conducting behaviour, depending on its lengths, the nature of the D/A system and the conformation. A result obtained for naphthyl- as donor and biphenyl- as acceptor is reported in Figure 12. We observe zero coupling at a dieder angle of 90 ° and a coupling of 8.2 cm^{-1} at 0 °. The electron transfer rate constant at an angle of 0 ° corresponds approximately to that expected for the c-hexane based bridge on the right side of Scheme VIII.

Scheme VIII

Marcus and Siddarth reported that the distance dependence of can be approximated as

$$H_{DA}^2 \propto e^{-\beta r_{DA}} \tag{5}$$

where r_{DA} is the distance between the Donor and the acceptor and β depends on the nature of the bridge and the D/A system. For c-hexane based bridges they found β = 0.9-1.0 Å^{-1}. We have calculated β = 0.85 Å^{-1} for the octasilasequioxane bridge. It would be very interesting to test these preliminary theoretical results by experiments. To do this, the substances must first be synthesized in pure form.

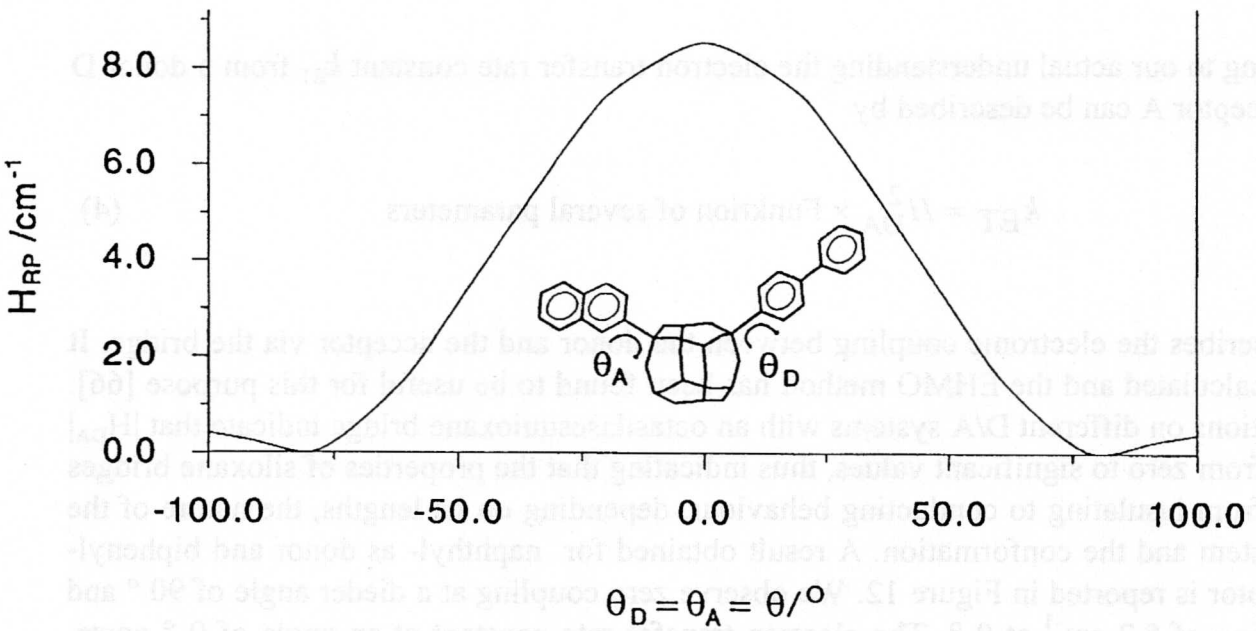

Figure 12: Electronic coupling term H_{DA} as a function of the dieder angle θ (θ_A=θ_D=θ). The plane of the aromatic rings is perpencicular to the plane of the top 4 Si atoms at θ=0.

Acknowledgements

This work was financed by the Schweizerischer Nationalfonds zur Förderung der wissenschaftlichen Forschung, project NF 20.040598.94/1, and by the Schweizerisches Bundesamt für Energiewirtschaft, project BEW (93)034.

References

[1] A. M. Bieniok, H.-B. Bürgi, *J. Phys. Chem.* **1994**, *98*, 10735.
[2] Y. I. Smolin, Y. F. Shepelev, R. Pomes, D. Hoebbel, W. Wieker, *Sov. Phys. Crystallogr.* **1979**, *24*, 19.
[3] E. J. Groenen, A. G. Kortbeek, M. Mackay, O. Sudmeijer, *Zeolites* **1986**, *6*, 403.
[4] Y. I. Smolin, Y. F. Shepelev, A. S. Ershov, D. Hoebbel, *Sov. Phys. Dokl.* **1987**, *32*, 943.
[5] G. Fu, C. A. Fyfe, W. Schwieger, G. T. Kototailo, *Angew. Chem. Int. Ed.* **1995**, *34*, 1499.
[6] M. Wiebcke, J. Emmer, J. Felsche, *J. Chem. Soc. Chem. Commun.* **1993**, 1604.
[7] N. Winkhofer, A. Voigt, H. Dorn, H. W. Roesky, A. Steiner, D. Stalke, A. Reller, *Angew. Chem.* **1994**, *106*, 1414.
[8] D.W. Scott, *J. Am. Chem. Soc.* **1946**, *68*, 356.
A.J.Barry, J.W. Gilkey, W.H. Daudt, J.J. Domicone, *J. Am. Chem. Soc.* **1995**, *77*, 4248.
[9] R. Müller, R. Köhne, S. Slivinski, *J. Prakt. Chem.* **1959**, 9, 71.
[10] K. Larsson, *Ark. Kemi* **1960**, *16*, 203, 209 and 215.
[11] M.G. Voronkov, V. I. Lavent'yev, *Top. Curr. Chem.* **1982**, *102*, 199.
E. Lukevics, O. Pudova, R. Sturkovich, *Molecular Structure of Organosilicon Compounds*, Ellis Horwood Limited, England, **1989**.
[12] R. Sasamori, Y. Okaue, T. Isobe, Y. Matsuda, *Science* **1994**, *265*, 1691.
[13] G. Calzaferri, *Nachr. Chem. Tech. Lab.* **1992**, *40*, 1106.
H. Bürgy, G. Calzaferri, D. Herren, A. Zhdanov, *Chimia* **1991**, *45*, 3.
[14] P. A. Agaskar, *Inorg. Chem.* **1991**, *30*, 2707.
[15] G. Calzaferri, R. Hoffmann, *J. Chem. Soc. Dalton Trans.* **1991**, 917.
[16] M. Bärtsch, P. Bornhauser, G. Calzaferri, R. Imhof, *J. Phys. Chem.* **1994**, *98*, 2817.
[17] P. Bornhauser, G. Calzaferri, *J. Phys. Chem.*, **1996**, *100*, 2035.
[18] V. W. Day, W. G. Klemperer, V.V. Mainz, D. M. Millar, *J. Am. Chem. Soc.* **1985**, *107*, 8262.
[19] H. Bürgy, G. Calzaferri, *Helv. Chim. Acta* **1990**, *73*, 698.
[20] D. Herren, H. Bürgy, G. Calzaferri, *Helv. Chim. Acta* **1991**, *74*, 24.
[21] G. Calzaferri, D. Herren, R. Imhof, *Helv. Chim. Acta* **1991**, *74*, 1278.
[22] G. Calzaferri, R. Imhof, *J. Chem. Soc. Dalton Trans.* **1992**, 3391.
[23] G. Calzaferri, R. Imhof, K. W. Törnroos, *J. Chem. Soc. Dalton Trans.* **1993**, 3741.
[24] C. Marcolli, R. Imhof, G. Calzaferri, *Microchim. Acta*, in press.
[25] B. Aebi, G. Calzaferri, D. Herren, R. Imhof, U.P. Schlunegger, *J. Mass Spec.*, submitted.
[26] B. J. Hendan, H. C. Marsmann, *J. Organomet. Chem.* **1994**, *483*, 33.
[27] U. Dittmar, B. J. Hedan, U. Flörke, H. C. Marsmann, *J. Organomet. Chem.* **1995**, *489*, 185.
[28] S. Lee, S. Makan, M. M. Holl, F. R. McFeely, *J. Am. Chem. Soc.* **1994**, *116*, 11819.
M. M. Holl, S. Lee, *Appl. Phys. Lett.* **1994**, *65*, 1097.
M. D. Nyman, S.B. Desu, C. H. Peng, *Chem. Mater.* **1993**, *5*, 1636.
M. M. Holl, F.R. McFeely, *Phys. Rev. Letters* **1993**, *71*, 2441.

[29] D. Hoebbel, I. Pitsch, T. Reiher, W. Hiller, H. Jancke, D. Müller, *Z. anorg. allg. Chem.* **1989**, *576*, 160.
D. Hoebbel, W. Wieker, *Z. anorg. allg. Chem.* **1971**, *384*, 43.
[30] D. Hoebbel, I. Pitsch, A. R. Grimmer, H. Jancke, W. Hiller, R. K. Harris, *Z. Chem.* **1989**, *29*, 260.
[31] F. J. Feher, J. J. Schwab, S. H. Phillips, Organometallics, in press.
F. J. Feher, T.A. Budzichowski, *J. Organomet. Chem.* **1989**, *379*, 33.
[32] P. A. Agaskar, *Synth. React. Inorg. Met.-Org. Chem.* **1990**, *20*, 483.
[33] P. A. Agaskar, *Inorg. Chem.* **1990**, *29*, 1603.
[34] F. J. Feher, K. J. Weller, *Inorg. Chem.* **1991**, *30*, 880.
[35] R. Tacke, A. Lopez-Mras, W. S. Sheldrick, A. Sebald, *Z. anorg. allg. Chem.* **1993**, *619*, 347.
[36] M. Morán, C. M. Casado, I. Cuadrado, J. Losada, *Organometallics* **1993**, *12*, 4327.
[37] A. R. Bassindale, T. E. Gentle, *J. Mater. Chem.* **1993**, *3*, 1319.
[38] P. Jutzi, C. Batz, A. Mutluay, *Z. Naturforsch.* **1994**, *49b*, 1689.
[39] R. Imhof, Ph.D. Thesis, Universität Bern, **1994**.
[40] G. Calzaferri, C. Marcolli, R. Imhof, K.W. Törnroos, J. Chem. Soc. Dalton Trans. 1996, 3313
[41] J. D. Lichtenhan, *Comments Inorg. Chem.* **1995**, *17*, 115.
[42] F. J. Feher, K. J. Weller, *Organometallics*, **1990**, *9*, 2638.
[43] F. J. Feher, K. J. Weller, J.J. Schwab, *Organometallics* **1995**, *14*, 2009.
[44] D. Herren, Ph.D. Thesis, Universität Bern, **1993**.
[45] F. J. Feher, K. J. Weller, *Chem. Mater.* **1994**, *6*, 7.
[46] I. Hasegawa, *Polyhedron* **1991**, *10*, 1097.
[47] D. Hoebbel, I. Pitsch, D. Heidemann, *Z. anorg. allg. Chem.* **1991**, *592*, 207.
[48] T. P. Auf der Heyde, H.-B. Bürgi, H. Bürgy, K. W. Törnroos, *Chimia* **1991**, *45*, 38.
[49] K.W. Törnroos, *Acta Cryst.* **1994**, *C50*, 1646.
[50] G. Calzaferri, C. Marcolli, J. Tomkinson, *ISIS Experimental Report, Rutherford Appleton Laboratory* **1995**.
[51] C. Marcolli, Ph.D. Thesis, Universität Bern, in preparation.
[52] M. Bärtsch, P. Bornhauser, G. Calzaferri, R. Imhof, *Vib. Spectrosc.* **1995**, *8*, 305.
[53] D. W. Turner, C. Baker, A. D. Baker, C. R. Brundle, *Molecular Photoelectron Spectroscopy*, Wiley-Interscience, London, **1970**.
[54] D.L. Griscom, *J. Non-Cryst. Solids* **1977**, *24*, 155.
[55] M. Brändle, G. Calzaferri, *Res. Chem. Intermed.* **1994**, *20*, 783.
[56] R. Beer, G. Calzaferri, J.-W. Li, B. Waldeck, *Coord. Chem. Rev.* **1991**, *111*, 193.
[57] G. Calzaferri, R. Giovanoli, I. Kamber, V. Shklover, R. Nesper, *Res. Chem. Intermed.* **1993**, *19*, 31.
[58] G. Calzaferri, N. Gfeller, K. Pfanner, *J. Photochem. Photobiol. A: Chemistry* **1995**, *87*, 81.
K. Pfanner, N. Gfeller, G. Calzaferri, *J. Photochem. Photobiol. A: Chemistry*, **1996**, *95*, 175.
[59] G. Calzaferri, A. Kunzmann, P. Lainé, K. Pfanner, *IS&T's 48th Annual Conference Proceedings*, Washington, D.C., May 7-11, **1995**, 318.
[60] G. Calzaferri, *Proceedings Photochemical and Photoelectrochemical Conversion and Storage of Solar Energy, IPS 9*, Editors Z. Wu Tien and Y. Cao, International Academic Publisher, Beijiing, **1993**, 141.
[61] G. Calzaferri, R. Imhof, K.W. Törnroos, *J. Chem. Soc. Dalton Trans.* **1994**, 3123.

[62] M. Bärtsch, G. Calzaferri, C. Marcolli, *Res. Chem. Interm.* **1995**, *21*, 577.
[63] R. A. Marcus, *Angew. Chem.* **1993**, *105*, 1161.
M. D. Newton, *Chem. Rev.* **1991**, *91*, 767.
[64] S. Larsson, J.M. Matos, *J. Mol. Struct.* **1985**, *120*, 35.
S. Larsson, *J. Am. Chem. Soc.* **1981**, *103*, 4034.
[65] M. D. Johnson, J. R. Miller, N. S. Green, G. L. Closs, *J. Phys. Chem.* **1989**, *93*, 1173.
[66] P. Siddarth, R. A. Marcus, *J. Phys. Chem.* **1990**, *94*, 2985.